PHYSICAL REVIEW B VOLUME 16, NUMBER 8 15 OCTOBER 1977

Hot-carrier effects in high magnetic fields in silicon inversion layers at low temperatures: p channel

Karl Hess
Ludwig Boltzmann Institut für Festkörperphysik und Institut für Angewandte Physik der Universität Wien, A-1090 Wien, Austria

T. Englert, T. Neugebauer, and G. Landwehr
Physikalisches Institut der Universität Würzburg, Würzburg, West Germany

G. Dorda
Siemens-Forschungslaboratorien, Munich, West Germany
(Received 8 April 1977)

A study of hot-carrier effects in the presence of high magnetic fields, in p-type silicon inversion layers is reported in a range of lattice temperatures between 1.25 and 20 K. Carrier temperatures T_c as a function of the electric field are deduced from measurements of the amplitude of Shubnikov–de Haas oscillations as a function of lattice temperature T_L ($T_L < 10$ K) and electric field E at high inversion-layer densities for the (110) orientation. For higher lattice temperatures, T_c is deduced from the classical magnetoresistance. In addition, measurements of the surface conductivity σ as a function of the source drain electric field at low hole concentrations, where σ depends on the temperature and the surface orientation, have been performed. It is found σ is proportional to E^s with $0 \le s \le 3$ over nearly two decades of E values.

I. INTRODUCTION

Space-charge layers at semiconductor surfaces are presently subject of careful theoretical and experimental investigations.[1-4] A p-type inversion layer is produced at the surface of an n-type semiconductor when the energy bands near the surface are bent so much that the top of the valence band lies near the Fermi level. The electric field perpendicular to the surface which is associated with the inversion layer is usually strong enough to group the energy levels of the charge carriers into electric subbands. When only the lowest subband is populated the charge carriers behave essentially as a two-dimensional gas. From the physical point of view it is primarily this two-dimensional nature and the possibility to change the surface charge carrier density at will which make the Si-SiO_2 system so interesting.

The structure of the electric subbands in the surface potential well has been determined by elaborate theoretical and experimental methods. The energy spacing between the subbands in n-type inversion layers has been investigated by optical absorption of far-infrared laser radiation.[5] The effective masses of holes have been determined from measurements of the Shubnikov–de Haas effect[6] and from cyclotron resonance.[7] The experimental results are in good agreement with theoretical predictions based on self-consistent calculations.[8] Thus the band structure of p-type inversion layers on the silicon surfaces seems fairly well understood.

In contrast to this, not too much is known about the phonons and the matrix element which describes the phonon-hole interaction.

Concerning the type of phonons several approaches towards the Si-SiO_2 interface have been considered:

(i) Kawaji[9] gave formulas for a strictly two-dimensional acoustic-phonon model (referred to as SK) and carrier-phonon interaction.

(ii) Ezawa[10] assumed that the elastic constants of Si and SiO_2 are sufficiently similar so that interface effects need not be taken into account. The charge carriers interact with bulk phonons in this case which is referred to as EKKN.

(iii) In a later publication by Ezawa[11] the elastic constants of SiO_2 are assumed to be so different from the constants of Si that surface waves are important for the carrier-phonon interaction. This case is later referred to as EKN.

(iv) In addition to these interactions with acoustic modes interactions with "optical phonons" having a very low Debye temperature Θ ($\Theta \approx 15$-50K) have been proposed by Krowne and Holm-Kennedy.[12]

Ezawa[11] considered first the Rayleigh mode only. In a later publication[13] other modes of surfons (the SV-P mode, the P-SV mode, etc.) have also been taken into account.

The problem to determine the interaction matrix element and phonon type is not trivial. A deduction from mobility measurements is not accurate enough, since the mobility is determined by surface roughness scattering and ionized impurity scattering, also. It has been shown, however,[14] that opti-

mal information about the interaction with phonons of low energy can be obtained from measurements of the energy loss of the charge carriers to the lattice[15] at low temperatures, because scattering by ionized impurities and surface roughness are elastic and do not contribute to the energy loss. The principle of energy-loss measurements is as follows.

The application of a high electric field E parallel to the surface results in a heating of the charge carriers above their thermal equilibrium value. After a time t (typically $10^{-12} \leq t \leq 10^{-7}$ sec) a stationary state is reached where the charge carriers gain power from the field at a rate $e\mu E^2$ and lose power at the same rate to the lattice.[15] The power loss at low temperatures depends mainly on the deformation potential Z_A and on the mean energy of the carriers. If their temperature T_c (which is of course higher than the lattice temperature T_L) is known, Z_A can be calculated.

In the following we present data for the energy loss of holes in silicon inversion layers as a function of the carrier temperature T_c at lattice temperatures $1.25 \leq T_L \leq 20$ K. These values have been deduced from measurements of the electric-field and temperature dependence of the amplitudes of Shubnikov–de Haas oscillations at $T_L \leq 10$ K and from the electric-field and temperature-dependent magnetoresistance at 10 K $\leq T_L$. The charge-carrier density was typically above $10^{12}/\mathrm{cm}^2$ in these experiments. Preliminary data have been presented elsewhere.[16]

Measurements of the field-dependent conductivity σ for lower carrier concentrations have also been performed. We found a power-law dependence $\sigma \propto E^s$ over a wide range of E values with the exponent s depending on the temperature.[17] A discussion of the results is given in Sec. III.

II. EXPERIMENTAL

Our aim was to determine the power loss rate as a function of the hole temperature T_c and at lattice temperatures $T_L < 20$ K. Because at higher temperatures[15] optical phonons with Debye temperatures $\Theta = 190$ and $\Theta = 650$ K are also important for the energy loss, the interpretation of the data becomes more difficult in this range.

In order to obtain information about the energy loss one has to measure some quantity $Q(T_L, E)$ as a function of T_L for a vanishing small field E and in addition as a function of E for constant lattice temperature T_L. Then a one-to-one correspondence of T_c to E can be established provided Q depends in the same way on T_L and on T_c. This is usually guaranteed if Q does not depend on the phonon-occupation number N_q.

For $T_L \leq 10$ K we used the amplitudes of the Shubnikov–de Haas (SdH) oscillations and for $T_L > 10$ K the transverse magnetoresistance $\Delta Q/Q_0$ as our quantity $Q(T_L, E)$. It was not possible to extend the SdH measurements to temperatures >10 K because the amplitudes of the quantum oscillations rapidly decrease with increasing temperature. However, in the overlap range the carrier heating deduced from both set of data agreed well—as expected. In order to avoid Joule heating of the lattice some of the experiments had to be performed using short current pulses. Typically, measurements were made 200 nsec after the beginning of the current pulse. The repetition rate of the current pulses was 40 sec^{-1}. No time dependence of the data was observed for 50 nsec $\leq t \leq 10$ μsec and repetition rates below 100 sec^{-1}.

For very low electric fields the pulsed signal was rather noisy. We therefore measured the SdH amplitudes with dc current also. Within the experimental error no differences have been observed in the low-field range between the pulsed and dc measurements. We also made sure in the following way that no lattice heating occurred: For low carrier concentration the sample resistance increases exponentially with T_L^{-1} with an activation energy of the order 1 meV or less. In this regime the resistance was measured with pulses and with dc methods as a function of temperature and electric field. From these data we found that dc and pulsed measurements agreed up to a certain power P_c supplied to the device (for our devices 0.1 mW). Consequently, all dc measurements were performed at lower power levels.

The devices were linear or circular transistors made on 8–10-Ω cm n-type silicon substrates having phosphorous doping of $\approx 2 \times 10^{15}/\mathrm{cm}^3$. The oxide thickness was 1.2×10^{-5} cm.

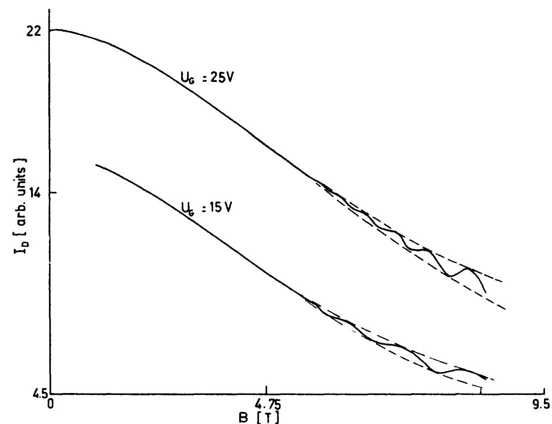

FIG. 1. Drain current vs magnetic field B for (I) $N_{\mathrm{inv}} = 1.6 \times 10^{12}/\mathrm{cm}^2$ ($U_G = 15$ V); (II) $N_{\mathrm{inv}} = 3.37 \times 10^{12}/\mathrm{cm}^2$ ($U_G = 25$ V).

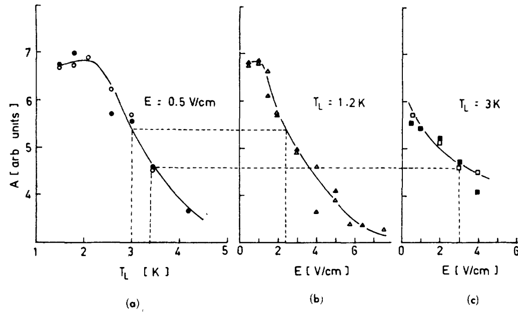

FIG. 2. Shubnikov–de Haas amplitudes (a) vs T_L at $E=0.5$ V/cm, (b) vs E for $T_L=1.2$ K, (c) vs E for $T_L=3$ K. ○, △, □: $N_{inv}=1.6\times10^{12}/\mathrm{cm}^2$; ●, ▲, ■: $N_{inv}=3.37\times10^{12}/\mathrm{cm}^2$.

Typical effective mobilities μ_{eff} at $T_L=4.2$ K were

$\mu_{eff}=300\ \mathrm{cm}^2/\mathrm{V\,sec}$ for (100) surfaces,

$\mu_{eff}=1200\ \mathrm{cm}^2/\mathrm{V\,sec}$ for (110) surfaces,

$\mu_{eff}=600\ \mathrm{cm}^2/\mathrm{V\,sec}$ for (111) surfaces,

at a hole concentration of $10^{12}/\mathrm{cm}^2$. The channel length was 4×10^{-3} cm.

Figure 1 shows the 4.2-K magnetoconductivity versus B at gate voltages $U_G=25$ V and 15 V, for a device with a (110) surface. The threshold voltage was about 6 V for $T_L\leq4.2$ K.

Devices with (100) and (111) surface orientation did not show SdH oscillations in the given range of magnetic fields, because the mobility was inadequate.

In Fig. 2(a) the SdH amplitudes at $B=8$ T are plotted versus temperature for a source-drain field strength of $E=0.5$ V/cm, and in Fig. 2(b) versus the electric field for $T_L=1.25$ K. The dotted line indicates the correspondence of temperature and field strength. Figure 2(c) shows the amplitudes versus E for $T_L=3$ K. These results are nearly independent of B. Note that the amplitudes vary much stronger with E for $T_L=1.25$ K than for $T_L=3$ K. The conductivity σ of the samples showed a small temperature and field dependence, also. In contrast to the SdH amplitudes the function $\sigma(E,T_L)$ differed from sample to sample and the E and T_L dependence was not even correlated for some of our devices, i.e., $\sigma(E,T_L)$ was increasing with E and decreasing with T_L and vice versa. This might be caused by contact effects or inhomogeneities. We will return to this point below.

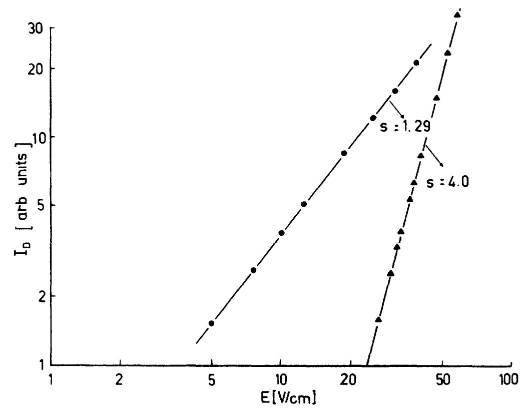

FIG. 4. $I_D(E,T_L)$ for (111) surface, $N_{inv}=8\times10^{11}/\mathrm{cm}^2$. $T_L=1.5$ K, ▲; $T_L=4.2$ K, ●.

At $T>10$ K the conductivity $\sigma(E,T_L)$ was the same for all samples measured and σ and the magneto-

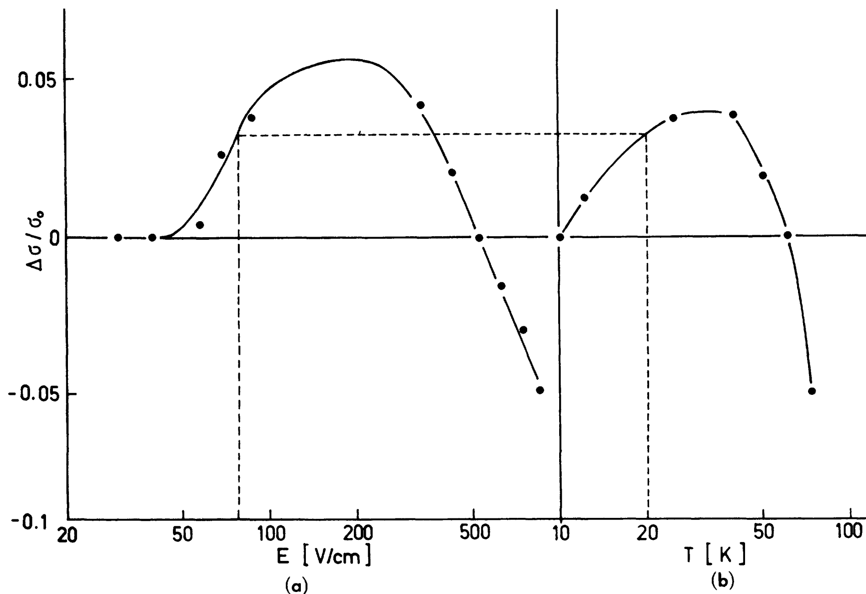

FIG. 3. Magnetoconductance ($N_{inv}=1.6\times10^{12}/\mathrm{cm}^2$) (a) vs E for $T_L=10$ K $=10$ K; (b) vs T_L for $E=0.5$ V/cm.

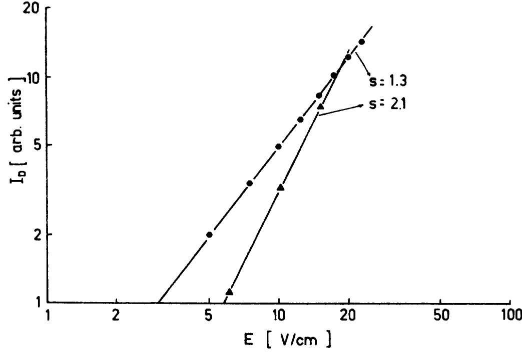

FIG. 5. $I_D(E, T_L)$ for (100) surface, $N_{\rm inv} = 8\times10^{11}/\mathrm{cm}^2$. $T_L = 1.5$ K, ▲; $T_L = 4.2$ K, ●.

conductance were correlated. The magnetoconductance

$$\Delta\sigma(E, T_L)/\sigma \equiv [\sigma(E, T_L; B = 6\mathrm{T}) - \sigma_0(E, T_L; 0)]/\sigma_0(E, T_L; 0)$$

is shown in Fig. 3(a) versus E for $T_L = 10$ K and in Fig. 3(b) versus T_L. Again a correlation can be found between E and T_L. These measurements were performed using short pulses, since the E values were very high in this case. For the experiments outlined above the carrier density was typically $10^{12}/\mathrm{cm}^2 \leq N_{\rm inv} \leq 6\times10^{12}/\mathrm{cm}^2$. The results reported are typical for the above given range of concentrations. For lower inversion layer hole densities the conductivity depends very strongly on both the temperature and electric field. The conductivity $\sigma(E, T_L)$ is shown in Fig. 4 for a typical (111) device and in Fig. 5 for typical (100) specimen for two different temperatures.

It can be seen that the conductivity follows a power law $\sigma(E, T_L) \propto E^s$ over a wide range of E values, with the exponent s dependent on temperature and surface orientation. Similar results were obtained previously.[17]

III. DISCUSSION

The energy loss $d\epsilon/dt$ of the carriers to the lattice by spontaneous emission of phonons has been discussed extensively in the literature.[15] It is given by the difference between the rates of phonon absorption and phonon emission, multiplied by the phonon energy, i.e.,

$$\frac{d\epsilon}{dt} = 2\pi \sum_{\vec q} \omega_{\vec q}\{|M_{\vec k,\vec k+\vec q}|^2[1 - f(\epsilon + \hbar\omega_{\vec q})] \times \delta(\epsilon_{\vec k+\vec q} - \epsilon_{\vec k} - \hbar\omega_{\vec q}) - |M_{\vec k,\vec k-\vec q}|^2[1 - f(\epsilon - \hbar\omega_{\vec q})] \times \delta(\epsilon_{\vec k-\vec q} - \epsilon_{\vec k} + \hbar\omega_{\vec q})\}. \quad (1)$$

The interaction matrix elements considered in the literature are

$$|M_{\vec k,\vec k'}|^2 = (Z_A^2\hbar q/2\rho_{2\,\mathrm{dim}} S u_1) \times (N_q + \tfrac12 \mp \tfrac12)\delta_{\vec k',\vec k\pm\vec q} \quad (2)$$

for the strictly two-dimensional theory[9];

$$|M_{\vec k,\vec k'}|^2 = \frac{Z_A^2 N(1-\gamma^2)q^2}{(\gamma q/b + 1)^6}(N_q + \tfrac12 \mp \tfrac12)\delta_{\vec k',\vec k\pm\vec q} \quad (3)$$

for Rayleigh waves (see the Appendix). For small $\gamma q/b$ ($T_c < 3$ K, $b \sim 10^7$ cm^{-1} $\gamma < 1$), this reduces to

$$|M_{\vec k,\vec k'}|^2 \propto q^2. \quad (4)$$

For $q/b \ll 1$, Eq. (4) holds also for the other surfon modes, which have been discussed by Ezawa.[13] For optical modes the matrix element is independent of q:

$$|M_{\vec k,\vec k'}|^2 = \mathrm{const}(N_R + \tfrac12 \mp \tfrac12)\delta_{\vec k',\vec k\pm\vec q}. \quad (5)$$

Here $\vec k$ and $\vec q$ are the wave vectors of holes and phonons, respectively; Z_A is the deformation potential constant; S is the area; $\rho_{2\,\mathrm{dim}} = \rho d \equiv 3\rho/b$; $\rho = 2.33\,g/\mathrm{cm}^3$ is the mass density of silicon; N_R is the phonon occupation number of the R mode of optical phonons; the constants N and γ are explained in the Appendix; d is the average spatial extension of the inversion layer; and u_1 is the sound velocity.

In EKKN interactions of electrons described by an envelope function used by Howard[1] with bulk phonons have been considered. The functional dependence of the corresponding matrix element on the phonon wave vector, however, is complicated. We will return to this point below. Explicit results for the energy loss have been obtained for the matrix element of Eq. (2) by assuming equipartition which means

$$N_q \approx k_B T_L/\hbar\omega_{\vec q}. \quad (6)$$

The sum in Eq. (1) is then easily performed and gives

$$\left\langle\frac{d\epsilon}{dt}\right\rangle = (2m^{*2}Z_A^2/\hbar^3\rho_{2\,\mathrm{dim}})k_B(T_L - T_c). \quad (7)$$

The large angular brackets indicate two-dimensional averaging over a Fermi distribution function with carrier temperature T_c.

For the interaction of electrons with Rayleigh waves no explicit expression can be given. Numerical calculations have been performed by Krowne and Holm-Kennedy,[12] which are in error, however.

If the phonon occupation number N_q cannot be approximated by Eq. (3), which is the case for a highly degenerate carrier gas, Eq. (1) has to be integrated numerically in any case. Extensive calculations show that

$$\lim_{T_c \to T_L} \left\langle \frac{d\epsilon}{dt} \right\rangle \propto (T_L - T_c) T_L^3/(\epsilon_F^3)^{1/2} \quad (8)$$

for the matrix element given by Kawaji[9] and

$$\lim_{T_c \to T_L} \left\langle \frac{d\epsilon}{dt} \right\rangle \propto (T_L - T_c) T_L^{p+2}/(\epsilon_F^3)^{1/2} \quad (9)$$

for matrix elements being proportional to $q^{p/2}$ (in addition to the $N_q + \frac{1}{2} \mp \frac{1}{2}$ dependence) and $\epsilon_F/k_B T_c \gtrsim 30$, where ϵ_F is the Fermi energy.

The power law in the temperature dependence is in close analogy to the dependence of the specific heat on T_L in the Debye theory[18] and arises from deviations from equipartition [Eq. (6)]. Measurements of the temperature dependence of the energy loss should allow one to distinguish the different scattering mechanisms. Dominating scattering of the holes by the mechanism described by Kawaji (strictly two dimensional) should lead to a T_L^3 dependence of the average energy loss, surfon scattering should result in a T_L^4 relation for $T_C - T_L$ much smaller than T_L and $T_L \to 0$. The parameter $\gamma q/b$ which is a measure for the penetration depth of the Rayleigh waves should be so small at low temperatures that it does not influence the temperature dependence of the energy loss.

As mentioned before the energy loss per carrier equals

$$\left\langle \frac{d\epsilon}{dt} \right\rangle = \sigma E^2/N_{\text{inv}} \equiv P \quad (10)$$

in the stationary state, which can be measured in a straightforward way. The experimental data were taken at transverse magnetic fields $B = 8$ T. For this field and hole concentrations of $N_{\text{inv}} = (1-3) \times 10^{12}/\text{cm}^2$, $\sigma/eN_{\text{inv}} \equiv \mu$ was found to be about 450 $\text{cm}^2/\text{V sec}$, nearly independent of temperature and electronic field. The carrier temperature T_c at a given electric field E can be extracted from our measurements as indicated in Figs. 3(a)–3(c) by the dotted line.

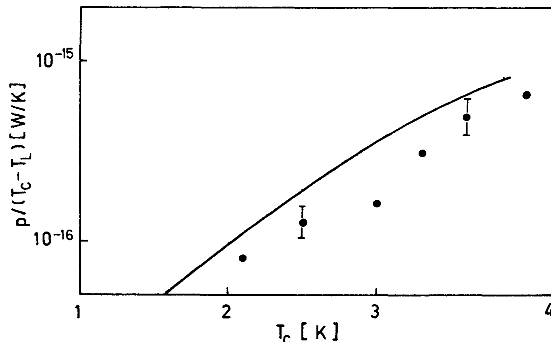

FIG. 6. Energy loss $P/(T_c - T_L)$ vs carrier temperature for $T_L = 1.25$ K. Full line, calculated; ●, experimental.

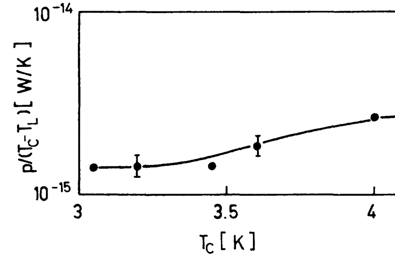

FIG. 7. Same as Fig. 6, but for $T_L = 3$ K.

It is now possible to plot the energy loss as a function of T_c and T_L. This has been done in Figs. 6–8 where $\langle d\epsilon/dt\rangle/(T_c - T_L) \equiv P/(T_c - T_L)$ has been plotted against T_c for $T_L = 1.25$, 3, and 10 K, and $N_{\text{inv}} = 1.6 \times 10^{12}/\text{cm}^2$. Figure 9 shows $P(\epsilon_F/24\ \text{meV})^{3/2}/(T_c - T_L)$ in the limit of $T_c - T_L \to 0$ as a function of lattice temperature. The limiting values of P are obtained by drawing a curve parallel to the theoretical (full lines) one through the experimental points, except for $T_L = 10$ K. Note, that for $T_L = 10$ K, the experimentally measured values for $P/(T_c - T_L)$ decrease with increasing carrier heating, whereas the theory predicts an increase. This can either be explained by the relatively large error bars of the experimental results in this temperature range or indicates a breakdown of the assumptions made in the calculations. The $P/(T_c - T_L)$ value taken in Fig. 9 was therefore the experimental result of Fig. 8 with T_c closest to T_L. The results obtained in this way follow closely at a T_L^4 law (full line in Fig. 9) and are not compatible with a T_L^3 relation as predicted by the strictly two-dimensional deformation potential theory. Scattering by optical phonons with low Debye temperature as proposed by Krowne and Holm-Kennedy would give an exponential T_L dependence and can be ruled out. Scattering by surfons, on the other hand, is compatible with the experimental results, as the T_L dependence of the EKKN mechanism (ordinary bulk phonons) has not yet been calculated. With the assumption of slightly broadened subband energy levels one may argue, however, that this mechanism gives the same T_L dependence as

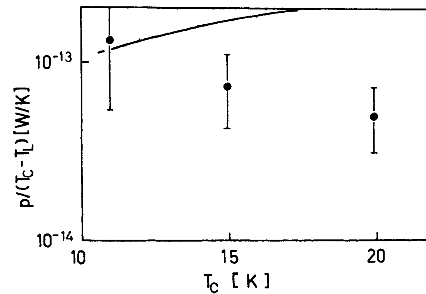

FIG. 8. Same as Fig. 6, but for $T_L = 10$ K.

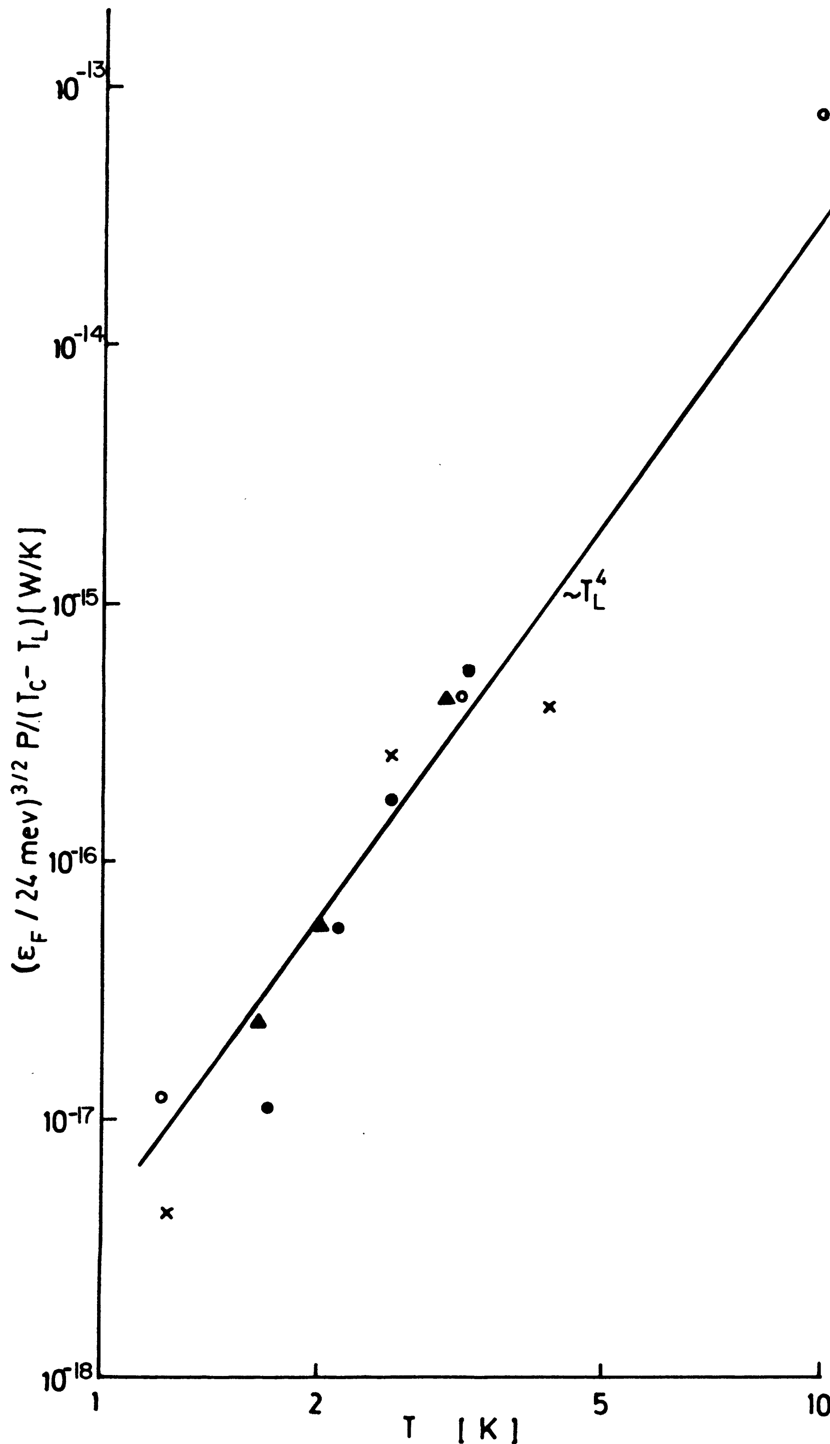

FIG. 9. Energy loss $P(\frac{1}{24}\epsilon_F\ \mathrm{meV})^{3/2}/(T_c - T_L)$ vs lattice temperature T_L for $T_c - T_L \ll T_c$; full line shows T_L^4 law. ▲, device 1: $N_{\mathrm{inv}} = 1.8 \times 10^{12}/\mathrm{cm}^2$; ○, device 2: $N_{\mathrm{inv}} = 1.6 \times 10^{12}/\mathrm{cm}^2$; ●, device 3: $N_{\mathrm{inv}} = 2.8 \times 10^{12}/\mathrm{cm}^2$; ×, device 4: $N_{\mathrm{inv}} = 2.3 \times 10^{12}/\mathrm{cm}^2$.

normal three-dimensional scattering in the bulk which yields a T_L^4 law. Thus the EKKN and the EKN mechanisms can probably not be distinguished.

Scattering by optical modes gives $d\epsilon/dt \propto \exp(\mathrm{const}/T_L)$. In order to calculate the absolute value of the energy loss to surfons one has to take into account also free carrier screening, possible disturbances of the phonon distribution, the complicated valence band structure and all the modes of surfons as given by Ezawa.[13] This is beyond the scope of this paper. However, the physical significance of our approach may be explored by con-

sidering only the Rayleigh mode and a spherical parabolical band structure with effective mass $m = 0.4m_0$. Using the sound velocities as given by Ezawa[13] we obtain the reasonable value of about 10 eV for Z_A. Krowne and Holm-Kennedy concluded in their paper[12] that surfon scattering is unimportant. They used, however, a matrix element which is in error by a factor $1/2\pi$.

The peculiar power law $I \sim E^s$ which is observed at low N_{inv} (Figs. 5 and 6) can certainly not be described in terms of hot carriers alone. Various groups have observed an activated behavior of the electrical resistivity[19-23] of silicon inversion layers at low temperatures and carrier concentrations below about $10^{12}/\text{cm}^2$. The resistivity increases exponentially with $1/T_L$ with the activation energy depending on the surface carrier concentration N_s.

Deviations from the exponential behavior can be produced[17] by increasing the source drain field strength to the order 1 V/cm. In addition it has been observed that at low source drain fields E, the magnetoconductivity behaves classically, whereas pronounced Shubnikov-de Haas oscillations show up at E values of the order 1 V/cm.

The available data can, at present, not be explained in a satisfying manner.[17,23] A model which assumes hopping between band tail states runs into difficulties because the hopping range would be of the order of 10^{-4} cm.[24] Moreover, the mobility which is derived from the classical magnetoresistance and from the onset of the Shubnikov-de Haas oscillations, is far larger than the effective mobility. It is also hard to reconcile the existence of a mobility edge with the existence of Shubnikov-de Haas oscillations.[17]

It has been proposed[21] that metallic and activated behavior can coexist and that the available data may be explained with a classical percolation model.

In order to check the percolation model, we have extended the measurements of the channel current as a function of the source drain field to higher electric field strengths of the order 100 V/cm. One would expect that at high field strengths the power law would break down.

Inspection of Figs. 4 and 5 shows, however, that the anomalous current voltage characteristics prevails at higher source drain fields. For the (111) device for which the data have been plotted in Fig. 4, exponents of 1.3 and 4.0 are found at temperatures of 4.2 and 1.5 K up to field strengths exceeding 50 V/cm. For the (100) device, the exponent found at 1.5 K turned out to be lower. In this case, we found $S = 2.1$. In some of the samples no correlation was found between the change in conductivity caused by carrier heating and by increasing the lattice temperature. This indicates, that—at least in some samples—"contact" effects and/or inhomogeneities must play a role.

We conclude that the new pulsed data for the activated range do not clarify the problem. It is hard to think of a mechanism which leads to a well-defined relation $I \propto E^s$, where s can be as high as 4 and depends strongly on temperature. So new efforts must be made in order to elucidate the transport properties in silicon inversion layers at low carrier concentrations.

APPENDIX: CALCULATION OF THE MATRIX ELEMENT FOR SCATTERING OF THE HOLES BY RAYLEIGH WAVES (SURFONS)

The lattice displacement was given by Ezawa[2]

$$\vec{U}_{\parallel}(\vec{R}) = \sum_{\vec{q}} i\sqrt{N}\,\frac{\vec{q}}{|q|}\left(e^{-\gamma q z} - \frac{2\gamma\eta}{1+\eta^2}\,e^{-\eta q z}\right) \times (a_{\vec{q}}\,e^{i\vec{q}\cdot\vec{\rho}} - \text{H.c.}), \tag{A1}$$

$$\vec{U}_{\perp}(\vec{R}) = -\sum_{\vec{q}} \vec{n}\sqrt{N}\left(\gamma e^{-\gamma q z} - \frac{2\gamma\eta}{1-\eta^2}\,e^{-\eta q z}\right) \times (a_{\vec{q}}e^{i\vec{q}\vec{\rho}} + \text{H.c.}), \tag{A2}$$

$$\vec{U}(\vec{R}) = \vec{U}_{\parallel}(\vec{R}) + \vec{U}_{\perp}(\vec{R}), \tag{A3}$$

here $(\vec{R})$ is a vector of ordinary space: (x, y, z); $\rho = (x, y, 0)$ is a vector parallel to the x-y surface plane; $\vec{n}$ is the unit vector perpendicular to the surface; $\vec{q}$ is the wave vector in the surface plane: $(q_x, q_y, 0)$; $\sqrt{N}$ is a normalization constant given below, and γ, η are functions of the Poisson ratio.[25] $\sqrt{N}$ has to be determined so that the Hamilton operator H becomes

$$H = \sum_{\vec{q}} \hbar c_R |\vec{q}|\,(a_{\vec{q}}^{\dagger} a_{\vec{q}} + \tfrac{1}{2}); \tag{A4}$$

this gives

$$N = \hbar/2S\rho_m c_R K(\sigma), \tag{A5}$$

where S is the surface area, c_R is the phase velocity of the Rayleigh wave, and

$$K(\sigma) = (\gamma - \eta)(\gamma - \eta + 2\gamma\eta^2)/2\gamma\eta^2, \tag{A6}$$

using

$$\Delta\epsilon = Z_A[\vec{\nabla}_R \cdot \vec{U}(R)]$$

for the modulation of the band edge by the sound wave (Z_A is the deformation potential), one easily obtains the matrix element

$$|M_{\vec{k}\vec{k}'}| = -\frac{Z_A\sqrt{N}q}{(\gamma q/b + 1)^3}\,(1 - \gamma^2)\,\delta_{\vec{k}',\vec{k}\pm\vec{q}} \times (N_q + \tfrac{1}{2} \mp \tfrac{1}{2})^{1/2}. \tag{A7}$$

*Measurements performed at the Physikalisches Institut der Universität Würzburg, supported by the Deutsche Forschungsgemeinschaft, the Ludwig Boltzmann Gesellschaft and the Fonds zur Förderung der wissenschaftlichen Forschung in Österreich No. 2576.

[1]F. Stern and W. E. Howard, Phys. Rev. 163, 816 (1967).
[2]G. Landwehr, Adv. Solid State Phys. 15, 49 (1975).
[3]F. Stern, Crit. Rev. Solid State Sci. 41, 499 (1944).
[4]G. Dorda, Adv. Solid State Phys. 15, 215 (1975).
[5]J. F. Koch, Adv. Solid State Phys. 15, 73 (1975).
[6]K. V. Klitzing, G. Landwehr, and G. Dorda, Solid State Commun. 14, 387 (1974); 15, 489 (1974).
[7]J. Kotthaus, Phys. Rev. B (to be published).
[8]See Ref. 2 and E. Bangert, Z. Phys. B (to be published); and F. J. Ohkawa and Y. Uemura, Prog. Theor. Phys. Suppl. 57, 164 (1975).
[9]S. Kawaji, J. Phys. Soc. Jpn. 27, 908 (1969).
[10]H. Ezawa, S. Kawaji, T. Kuroda, and K. Nakamura, Surf. Sci. 24, 659 (1971).
[11]H. Ezawa, T. Kuroda, and K. Nakamura, Surf. Sci. 24, 654 (1971).
[12]C. M. Krowne and J. W. Holm-Kennedy, Surf. Sci. 46, 232 (1974).
[13]H. Ezawa, S. Kawaji, and K. Nakamura, Jpn. J. Appl. Phys. 13, 126 (1974).
[14]F. F. Fang and A. B. Fowler, J. Appl. Phys. 41, 1825 (1970).
[15]K. Hess and C. T. Sah, Phys. Rev. B 10, 3375 (1974).
[16]K. Hess, Th. Englert, T. Neugebauer, G. Landwehr, and G. Dorda, Proceedings of the Thirteenth International Conference on the Physics of Semiconductors, Roma, 1976 (unpublished), p. 746.
[17]See also, Th. Englert and G. Landwehr, Surf. Sci. 58, 217 (1976).
[18]C. Kittel, *Solid State Physics* (Wiley, New York, 1965), p. 125.
[19]H. Pepper, S. Pollitt, and C. J. Adkins, Phys. Lett. A 47, 71 (1974); 48, 113 (1974).
[20]D. C. Tsui and S. J. Allen, Jr., Phys. Rev. Lett. 32, 1200 (1974).
[21]E. Arnold, Appl. Phys. Lett. 25, 709 (1974); and Surf. Sci. 58, 60 (1970).
[22]M. E. Sjöstrand and P. J. Stiles, Solid State Commun. 16, 903 (1975).
[23]S. J. Allen, D. C. Tsui, and F. de Rosa, Phys. Rev. Lett. 35, 1359 (1975).
[24]N. F. Mott and E. A. Davis, *Electronic Processes in Non-Crystalline Materials* (Clarendon, Oxford, 1971), p. 266.
[25]H. Ezawa, Ann. Phys. (Leipz.) 67, 438 (1971).